The 2012 IEEE/ASME International Conference on
Advanced Intelligent Mechatronics
July 11-14, 2012, Kaohsiung, Taiwan

Analysis for Configuration Prediction of Redundant Manipulators based on AMSIP Distribution

Yang Hou, Akira Yanou, Mamoru Minami, Yosuke Kobayashi and Satoshi Okazaki

***Abstract*— This paper proposes and analyses an approach named predictive control of redundant manipulators based on Avoidance Manipulability Shape Index with Potential (AMSIP), which is an evaluation index considering avoidance manipulability and collision possibility, in order to achieve an on-line control of trajectory tracking and obstacle avoidance for redundant manipulators. In the trajectory tracking process, manipulator is required to keep a configuration with maximal avoidance manipulability in real time. Predictive control in this paper uses manipulators' future configurations to control current configuration aiming at completing tasks of trajectory tracking and obstacle avoidance on-line and simultaneously with higher avoidance manipulability. We compare Multi-Preview Control with Predictive Control using redundant manipulator, and show the results through simulations. Moreover, we validate the effectiveness of Predictive Control through AMSIP distribution.**

I. INTRODUCTION

Over the past two decades, redundant manipulators were used for various tasks, for example, welding, sealing and grinding. These kinds of tasks require that the manipulator plans its hand onto a desired trajectory (trajectory tracking) and avoid its intermediate links, meaning all comprising links of robot except the top link with the end-effector, from obstacles existing near the target object and also the target object itself (obstacle avoidance).

Multi-Preview Control can refer to many shapes of manipulator optimized by avoidance manipulability to induce the current manipulator's shape [1], and avoid collisions with the obstacles. However, because Multi-Preview Control can not immediately compensate the error when manipulator is tracking trajectory or avoiding obstacle, there are still existing possible situations that manipulator could not avoid collision effectually. Moreover in actual working situation, oscillation or overshoot on the tracking trajectory of manipulator's hand may occur because manipulator has dynamics. The features of our system are shown in Fig.1 where the camera scene area symbolizes the restricted information of environment.

For these problems, the prediction of manipulators' future configuration has possibility of effectively compensating a tracking error. In other words, predictive control of redundant manipulator considering avoidance manipulability may realize fast and precision working. Although the effectiveness of predictive control is confirmed in the case of straight line target trajectory[2],[3], it is not confirmed in the case of curve target trajectory. Therefore this paper explores the

Yang Hou, Akira Yanou, Mamoru Minami, Yosuke Kobayashi and Satoshi Okazaki are with Graduate School of Natural Science and Technology, Okayama University Tsushimanaka3-1-1 , Okayama, Japan. houyang, yanou, minami, kobayashi2, okazakis@suri.sys.okayama-u.ac.jp.

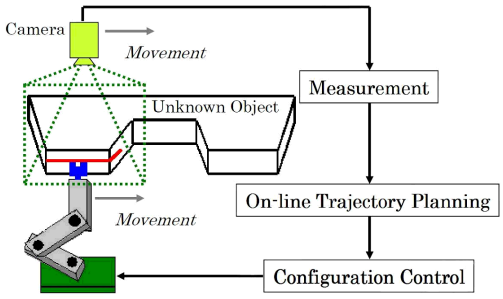

Fig. 1. Processing system for unknown object

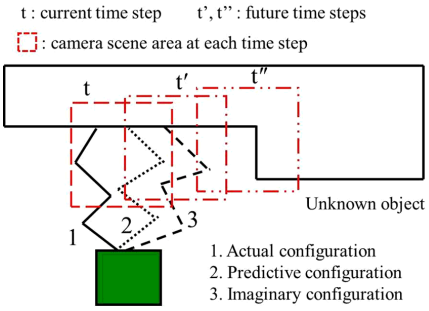

Fig. 2. Concept of predictive control

effectiveness of future configuration prediction of redundant manipulator onto curve trajectory based on AMSIP distribution. Although predictive control[4] has been widely applied in the industry field, the main target is seemed to be trajectory tracking and not a configuration control of robot manipulator. On the other hand, there are interesting researches on trajectory tracking and configuration control of robot by [5] using rapid exploring random trees, [6] using path searching and pruning algorithm, and so on. This paper also deals with trajectory tracking and configuration control of manipulator, and the difference from their methods is the use of predictive values of manipulator's configuration due to approaching actual manipulator's configuration to imaginary manipulator's configuration with on-line calculation of high AMSIP[7] value using 1-step GA[8]. And also the proposed method assumes that the collision avoidance problem in unstructured and dynamic environment is included as shown in Fig.2. In other words, the future reference trajectory is unknown and therefore it is noticed that the problem has to been solved on-line and adaptively in limited recognition time. In order to make the manipulator avoid obstacles

and track working object successfully, we have defined the AMSIP [7] and we have proposed multi-preview control method which based on 1-step Genetic Algorithm (1-step GA) (please refer to [8] about the detail of 1-step GA) to calculate the future configuration of imaginary manipulator. About the redundant part $\boldsymbol{l}(t)$ which denotes in control formula of multi-preview control, we have proposed a concept named predictive control which based on future time to make the configuration of imaginary manipulator and the predictive configuration of actual manipulator closer. It also means that the actual configuration will be closer to the imaginary configuration to keep high avoidance manipulability by using predictive configuration as shown in Fig.2. However, the configuration of actual manipulator sometimes cannot be predicted prosperously, and the manipulability degree cannot be predicted correctly. In this paper, we have analyzed the correctness of configuration prediction of second order approximation onto straight trajectory and curve trajectory through simulation, and we also want to compare multi-preview control with predictive control by using AMSIP distribution.

II. AVOIDANCE MANIPULABILITY SHAPE INDEX WITH POTENTIAL

We proposed Avoidance Manipulability Ellipsoid and Avoidance Manipulability Shape Index (AMSI) in [9], and Avoidance Manipulability Shape Index with Potential (AMSIP) in [7]. Avoidance Manipulability Ellipsoid is applied from Manipulability Ellipsoid proposed by Prof. Yoshikawa in [10]. We will elucidate them briefly in this section.

When the desired hand velocity $\dot{\boldsymbol{r}}_{nd}$ is given, $\dot{\boldsymbol{q}}_n$ is solved as

$$\dot{\boldsymbol{q}}_n = \boldsymbol{J}_n^+ \dot{\boldsymbol{r}}_{nd} + (\boldsymbol{I}_n - \boldsymbol{J}_n^+ \boldsymbol{J}_n)\ {}^1\boldsymbol{l}, \tag{1}$$

where $\boldsymbol{J}_n^+$ is the pseudo-inverse of Jacobean Matrix $\boldsymbol{J}_n$ and $\boldsymbol{I}_n$ is a $n \times n$ unit matrix. In addition, ${}^1\boldsymbol{l}$ is an arbitrary vector. Trajectory tracking of the hand and collision avoidance can executed simultaneously through this vector ${}^1\boldsymbol{l}$. Here, control variable ${}^1\boldsymbol{l}$ is determined so as to make actual manipulator's shape at current time $\boldsymbol{q}(t)$ close to future optimal shape by referring to the future optimal shapes of imaginary manipulators.

The relation of the desired velocity of the i-th link ${}^1\dot{\boldsymbol{r}}_{id}$ and the desired hand velocity $\dot{\boldsymbol{r}}_{nd}$ is shown in Eq.(2).

$${}^1\dot{\boldsymbol{r}}_{id} = \boldsymbol{J}_i \boldsymbol{J}_n^+ \dot{\boldsymbol{r}}_{nd} + \boldsymbol{J}_i (\boldsymbol{I}_n - \boldsymbol{J}_n^+ \boldsymbol{J}_n)\ {}^1\boldsymbol{l} \tag{2}$$

Here we define two variables shown in Eq.(3) and Eq.(4).

$$\Delta^1\dot{\boldsymbol{r}}_{id} \stackrel{\triangle}{=} {}^1\dot{\boldsymbol{r}}_{id} - \boldsymbol{J}_i \boldsymbol{J}_n^+ \dot{\boldsymbol{r}}_{nd}, \tag{3}$$

$${}^1\boldsymbol{M}_i \stackrel{\triangle}{=} \boldsymbol{J}_i (\boldsymbol{I}_n - \boldsymbol{J}_n^+ \boldsymbol{J}_n). \tag{4}$$

According to Eq.(2),Eq.(3) and Eq.(4), $\Delta^1\dot{\boldsymbol{r}}_{id}$ can be rewritten as

$$\Delta^1\dot{\boldsymbol{r}}_{id} = {}^1\boldsymbol{M}_i\ {}^1\boldsymbol{l}. \tag{5}$$

In Eq.(5), $\Delta^1\dot{\boldsymbol{r}}_{id}$ is called the first avoidance velocity and ${}^1\boldsymbol{M}_i$ is a $m \times n$ matrix called the first avoidance matrix.

Next, we will represent the Avoidance Manipulability Ellipsoid. Providing that ${}^1\boldsymbol{l}$ is restricted as $\|{}^1\boldsymbol{l}\| \leq 1$, then the extent where $\Delta^1\dot{\boldsymbol{r}}_{id}$ can move is denoted as

$$\Delta^1\dot{\boldsymbol{r}}_{id}^T ({}^1\boldsymbol{M}_i^+)^T\ {}^1\boldsymbol{M}_i^+ \Delta^1\dot{\boldsymbol{r}}_{id} \leq 1. \tag{6}$$

If $rank({}^1\boldsymbol{M}_i) = m$, the ellipsoid represented by Eq.(6) is named as the first complete avoidance manipulability ellipsoid. If $rank({}^1\boldsymbol{M}_i) = p < m$, the ellipsoid is named as the first partial avoidance manipulability ellipsoid.

The volume of each Avoidance Manipulability Ellipsoid indicates mobility of each link (shape-changeability). The larger total volume indicates the higher whole avoidance manipulability. We evaluated total volume as Avoidance Manipulability Shape Index (AMSI). Then we proposed Avoidance Manipulability Shape Index with Potential (AMSIP) which considers AMSI and the distance between the manipulator and target object. And we verified the superiority of AMSIP through the simulation in [7].

III. MULTI-PREVIEW CONTROL

Multi-Preview Control controls current manipulator's shape by referring several imaginary manipulator's shape at several future times. As shown in Fig.3, Multi-Preview Control System consists of an on-line measurement block, a path planning block, a redundancy control block and redundant manipulator. On the assumption that current time is represented by t, and the future times are defined as $t_i^* = t + i\tilde{t}$, $(i \in [1, p])$ where $\tilde{t}$ denotes preview time and i is the number of future times. A measurement block detects a desirable hand position $\boldsymbol{r}_d(t_i^*)$ on the surface of the target object at time t_i^*, which is reasonably assumed to be possible to detect the future information only in the detected camera image in Fig.3. Firstly, potential space based on the detected shape of the target object is created around it at the path planning block. Then the path planning block outputs the optimal shape $\tilde{\boldsymbol{q}}_d(t_i^*)$ corresponding to the maximum ${}^1S$ presented in [1] at the future time t_i^* (imaginary manipulator) by 1-Step GA. The control block outputs desired joint angular velocity $\dot{\boldsymbol{q}}_d(t)$ that makes actual manipulator's shape at current time $\boldsymbol{q}(t)$ close to the optimal shape in the future by referring to $\sum_{i=1}^{p} \tilde{\boldsymbol{q}}_d(t_i^*)$.

An equation which realizes this control system is named as Preview Control equation and expressed as follows

$$\dot{\boldsymbol{q}}_d \quad = \quad \boldsymbol{J}_n^+ \dot{\boldsymbol{r}}_{nd} + (\boldsymbol{I}_n - \boldsymbol{J}_n^+ \boldsymbol{J}_n)\boldsymbol{l}(t) \tag{7}$$

where $n \times 1$ matrix $\boldsymbol{l}(t)$ is defined as

$$\boldsymbol{l}(t) = \boldsymbol{K}_v \Big(\sum_{i=1}^{p} \tilde{\boldsymbol{q}}_d(t_i^*) - \boldsymbol{q}(t)\Big) = \begin{bmatrix} \sum_{i=1}^{p} \tilde{q}_{1d}(t_i^*) - q_1(t) \\ \vdots \\ \sum_{i=1}^{p} \tilde{q}_{jd}(t_i^*) - q_j(t) \\ 0 \\ \vdots \\ 0 \end{bmatrix} \tag{8}$$

when redundant degrees j remains and the redundancy is used for the joints from 1 to j.

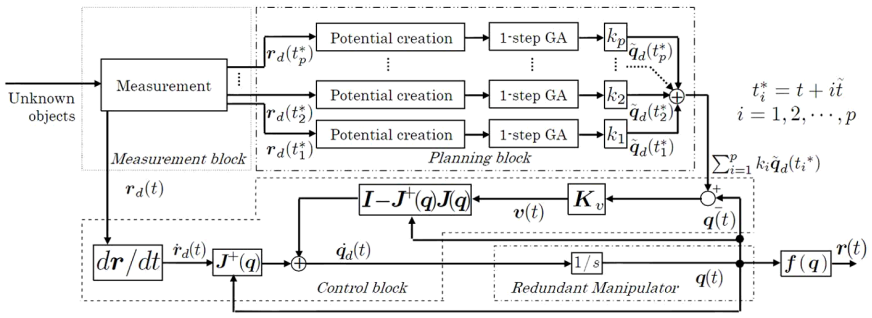

Fig. 3. Multi-Preview Control system

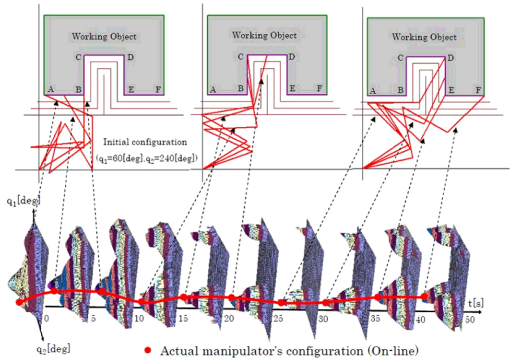

Fig. 4. Actual manipulator's configurations in whole tracking process based on multi-preview control

The transition of AMSIP and the manipulator's shape using Multi-Preview Control System is shown in Fig.4. According to Fig.4, we can find that the manipulator can always keep higher AMSIP value by using Multi-Preview Control. And the AMSIP value obtained by this system moves from one higher peak to another higher peak as time in multi peak AMSIP distributions. This verifies the validity of multi-preview control in 2-dimension by 4-link planar manipulator.

IV. PREDICTIVE CONTROL METHOD

We used predictive value of manipulator's configuration in preview control equation. In order to make the actual manipulator's posture be closer to the future configuration of imaginary manipulator, we changed the $\boldsymbol{l}(t)$ of the second part of multi-preview's control equation as follow.

$$\boldsymbol{l}(t) = \boldsymbol{K_v} \sum_{i=1}^{p} k_i \Big(\tilde{\boldsymbol{q}}_d(t_i^*) - \widehat{\boldsymbol{q}}(t_i^*) \Big) \tag{9}$$

We thought that the $\widehat{\boldsymbol{q}}(t_i^*)$ is the future configuration's predictive value of manipulator. And in our research, we gave the following Eq.(10) because we define $t_i^* = t + i{\cdot}\tilde{t}$ in the previous section.

$$\boldsymbol{q}(t_i^*) = \boldsymbol{q}(t + i{\cdot}\tilde{t}), (i = 1, 2, \cdots, p) \tag{10}$$

After using Taylor expansion to calculate the predictive value $\widehat{\boldsymbol{q}}(t_i^*)$, then following equation Eq.(11), which is second approximation of Taylor expansion, could be derived,

$$\boldsymbol{q}(t + i{\cdot}\tilde{t}) \approx \boldsymbol{q}(t) + i{\cdot}\tilde{t}\dot{\boldsymbol{q}}(t) + \frac{1}{2}(i{\cdot}\tilde{t})^2 \ddot{\boldsymbol{q}}(t) \tag{11}$$

To the differential part in Eq.(11), we did approximate calculation by using Eq.(12) and Eq.(13).

$$\dot{\boldsymbol{q}}(t) \approx \frac{\boldsymbol{q}(t) - \boldsymbol{q}(t-h)}{h} \tag{12}$$

$$\ddot{\boldsymbol{q}}(t) \approx \frac{\dot{\boldsymbol{q}}(t) - \dot{\boldsymbol{q}}(t-h)}{h} \tag{13}$$

Where h is a tiny value. Based on the above equations, we did second approximate calculation to the Taylor expansion for manipulations' future configuration value, and after replacing the differential term of Eq.(11) by Eq.(12) and Eq.(13), we can derive the predictive equation $\widehat{\boldsymbol{q}}(t_i^*)$ of actual manipulators' configuration as follow. In this paper, it is noticed that the predictive equation $\widehat{\boldsymbol{q}}(t_i^*)$ does not include the manipulators' dynamics.

$$\begin{aligned} \widehat{\boldsymbol{q}}(t_i^* \mid t) \;=\; & \Big(1 + \frac{i{\cdot}\tilde{t}}{h} + \frac{1}{2}(\frac{i{\cdot}\tilde{t}}{h})^2\Big)\boldsymbol{q}(t) - \Big(\frac{i{\cdot}\tilde{t}}{h} + (\frac{i{\cdot}\tilde{t}}{h})^2\Big) \\ & {\cdot}\boldsymbol{q}(t-h) + \frac{1}{2}(\frac{i{\cdot}\tilde{t}}{h})^2 \boldsymbol{q}(t-2h) \end{aligned} \tag{14}$$

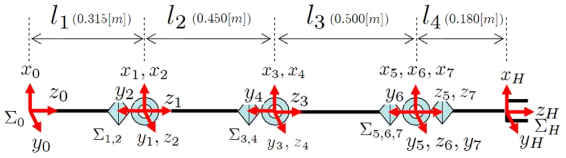

Fig. 5. Coordinate System of PA10

V. SIMULATION

In order to compare the multi-preview control with predictive control, we use a 7-link manipulator for simulations, which is produced by Mitsubishi Heavy Industries named PA10 and the structure of PA10 is shown in Fig.5.

A. Case of straight trajectory

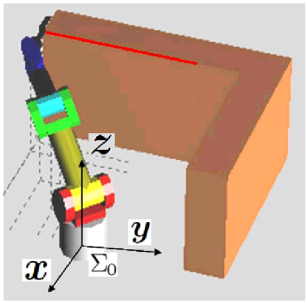

Fig. 6. Outside appearance of simulation

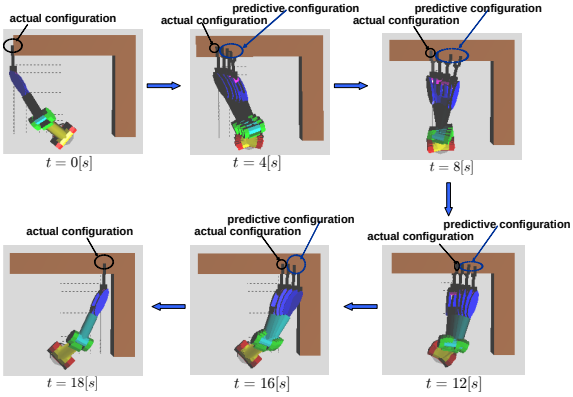

Fig. 7. Screen shot of simulation

Hand tracking trajectory and given manipulator's shape are depicted in Fig.6, target hand trajectory is predefined. In addition, the kinematics of PA10 is implemented in the simulator. The solid line in Fig.6 expresses a reference trajectory set to be followed. The simulation's screen shot is shown in Fig.7.

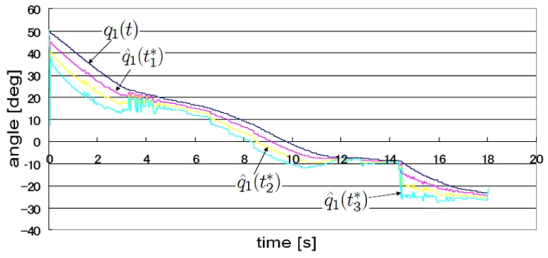

Fig. 8. Actual and predictive angle of link 1 ($\tilde{t}$=0.6[s])

The angle of actual manipulators' link 1 and the predictive angles $\hat{q}_1(t_1^*)$, $\hat{q}_1(t_2^*)$, $\hat{q}_1(t_3^*)$ of manipulators' link 1 is indicated in Fig.8. The angle of actual manipulators' link 2 and the predictive angles $\hat{q}_2(t_1^*)$, $\hat{q}_2(t_2^*)$, $\hat{q}_2(t_3^*)$ of it is indicated in Fig.9. Moreover, we use Runge-Kutta method to calculate current angle of actual manipulator in simulation, the interval time h of Runge-Kutta is 0.03 [s], and the value h also be

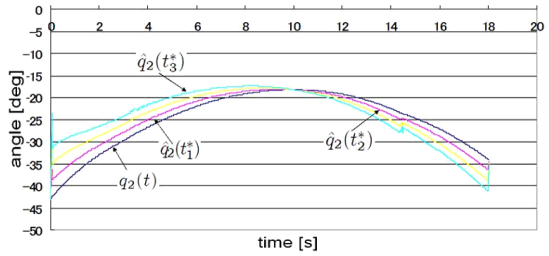

Fig. 9. Actual and predictive angle of link 2 ($\tilde{t}$=0.6[s])

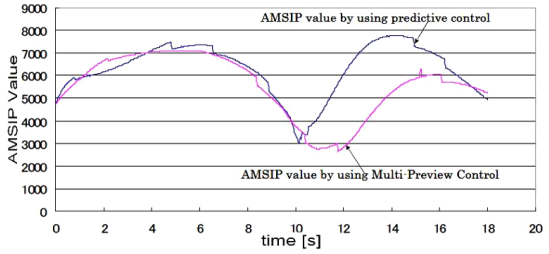

Fig. 10. AMSIP value

used in Eq.(14). Obviously, the posture of manipulator could be closer to the future configuration expressed by predictive values. We thought that actual manipulators' posture could be forecasted effectively by using predictive control.

Furthermore, we got the AMSIP average of actual manipulator's posture by using multi-preview control and predictive control by fifteen times respectively, and indicated the average values by time t in Fig.10. Compared with Multi-Preview Control, we believe that AMSIP value can maintain a higher value by using predictive control. Through simulations, we also thought predictive control has a possibility to be superior to multi-preview control.

We investigated the manipulability degree $\omega(\boldsymbol{q}(t))$ of actual angles $\boldsymbol{q}(t)$ and the predictive angles $\hat{\boldsymbol{q}}(t_1^*)$, $\hat{\boldsymbol{q}}(t_2^*)$, $\hat{\boldsymbol{q}}(t_3^*)$ of manipulators based on Eq.(15), and showed the result by Fig.11, according to predictive interval time is 0.6[s].

$$\omega(\boldsymbol{q}(t)) = \sqrt{det\boldsymbol{J}_n(\boldsymbol{q}(t))\boldsymbol{J}_n^T(\boldsymbol{q}(t))} \tag{15}$$

Observed Fig.11, we obviously can believe that predictive control can also predict the manipulability degree of manipulator. However, in Fig.9, when t=7.5 and t=9.5, the value of manipulability degree get large suddenly, and manipulability degree become difficult to be predicted. About this problem, we also need to do further study.

B. Case of curve trajectory

We want to know the manipulator will be predicted effectively or not when the trajectory is curve trajectory, The solid line in Fig.12 expresses a target curve trajectory set to be followed. The angle of actual manipulators' link 1 and the predictive angles $\hat{q}_1(t_1^*)$, $\hat{q}_1(t_2^*)$, $\hat{q}_1(t_3^*)$ of manipulators' link 1 is indicated in Fig.13 when predictive interval time

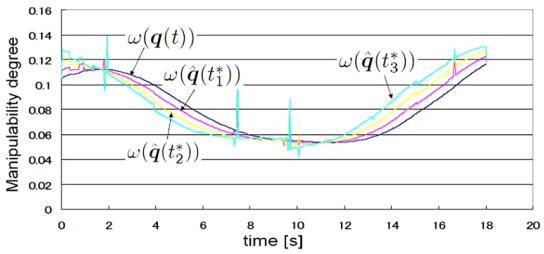

Fig. 11. Manipulability degree ($\tilde{t}$=0.6[s])

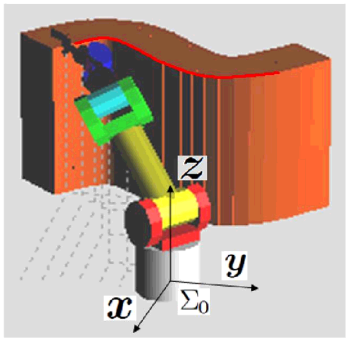

Fig. 12. Outside appearance of simulation

is 0.6[s]. The angle of actual manipulators' link 2 and the predictive angles $\hat{q}_2(t_1^*)$, $\hat{q}_2(t_2^*)$, $\hat{q}_2(t_3^*)$ of it is indicated in Fig.14 when predictive interval time is 0.6[s]. we believe that the posture of manipulator could be closer to the future configuration expressed by predictive values. We thought that actual manipulators' posture could be forecasted effectively by using predictive control in the curve trajectory. However, because the actual manipulators' angular velocity of link1 and link2 are not smooth, so sometimes the predictive lines are also not smooth enough.

We show the manipulability degree by Fig.15 when predictive interval time is 0.6[s]. we obviously can believe that predictive control can also predict the manipulability degree of manipulator. However, we think the prediction result is better when predictive interval time is smaller. Because the predictive lines in Fig.15 is not smooth enough, so we think the manipulability degree is hard to be predicted when predictive interval time is 0.6[s].

Finally, we want to check the effectiveness of predictive control for curve trajectory. In this paper we got the AMSIP value average of actual manipulator's posture by using multi-preview control and predictive control when the trajectory is curve trajectory, and indicated the average values by time t in Fig.16. Compared with multi-preview control, we believe that AMSIP value can also maintain a higher value by using predictive control. Through simulations, it can find that predictive control has a possibility to be superior to multi-preview control even if the target trajectory is curve.

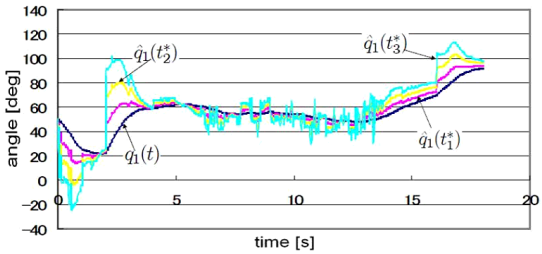

Fig. 13. Actual and predictive angle of link 1 ($\tilde{t}$=0.6[s])

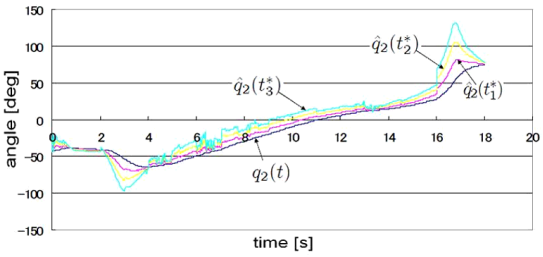

Fig. 14. Actual and predictive angle of link 2 ($\tilde{t}$=0.6[s])

VI. AMSIP DISTRIBUTION

We examine the AMSIP value distribution in a whole sphere of redundant degrees based on a straight target object's shape. Since the AMSIP distribution relies on both target object's shape and the redundant manipulator's shape, we need to assume a given target objects form and also a predetermined manipulator's structural configuration. The working space dimension of the manipulator's hand task is set to be 5, where position dimension is 3 and posture dimension is 2. Then the manipulator has 2 redundant DoF because PA10 has 7 DoF. And we give this 2 redundant DoF to 1-st joint, q_1, and 2-nd joint, q_2. Through inverse kinematics of PA10, we can determine q_3 to q_7 from desired hand trajectory and q_1, q_2 given by preview control.

Concerning AMSIP value distribution, a high AMSIP value means that the manipulator has higher shape-changeability and keeps distance between its links and the working object (obstacle) to be safe. That, in Fig.17, when AMSIP value equals 0 (color is black) means there cannot exist inverse kinematics solution to use redundancy, when AMSIP value isn't 0 (color isn't black) means there can exist high avoidance manipulability. In Fig.17, we named the bottom left circle as A, and the higher right circle as B. The numbers put on whites points of the colored circle correspond shapes of the manipulator, which are showed in Fig.18 and Fig.19. The two circles of A and B indicates separate possible configurations represented in Fig.18 and Fig.19. Please notice the ① $\sim$ ⑥ in the Fig.17 corresponds to the number of the shapes in Fig.18 and Fig.19. Seeing A-shapes and B-shapes of the manipulator in sequence of ① $\sim$ ⑥, we can understand that, firstly, hand's posture is controlled by given desired fixed value, secondly, the redundancy is used for arbitrary position of the elbow, thirdly,

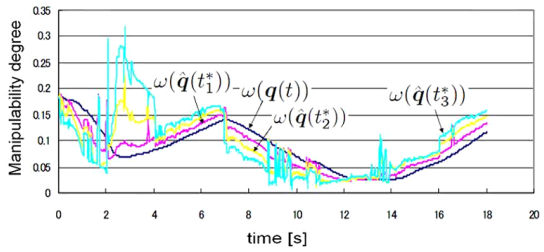

Fig. 15. Manipulability degree ($\tilde{t}$=0.6[s])

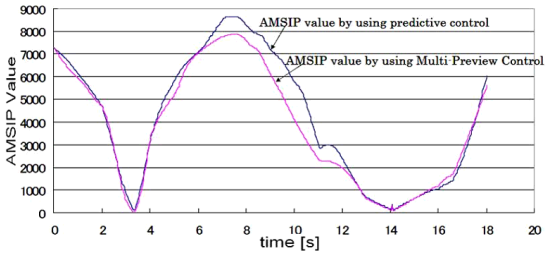

Fig. 16. AMSIP value

the corresponding configurations of A and B are identical. In a word, the configurations of manipulators can be expressed by Fig.17.

In Fig.20, the white circle means actual manipulator, the blue circle means predictive manipulator 1 ($\hat{\boldsymbol{q}}(t_1^*)$), the green circle means predictive manipulator 2 ($\hat{\boldsymbol{q}}(t_2^*)$), the pink circle means predictive manipulator 3 ($\hat{\boldsymbol{q}}(t_3^*)$), and the configurations of manipulators have shown in redundance space and also shown by Fig.21, in Fig.21, predictive manipulator 1, predictive manipulator 2, and predictive manipulator 3 are same with predictive manipulators in Fig.20.

We show AMSIP value distribution from Fig.20 to Fig.33 in case of predictive control. The predictive interval time $\tilde{t}$ is 1.2 [s]. In this simulation, we set k_1=0.1, k_2=0.2, k_3=0.7. From Fig.20 to Fig.33, we think that the actual manipulator's configuration is close to predictive manipulators' configuration. We show AMSIP value distribution by Fig.35 to Fig.40 in case of Multi-Preview Control from t=0 to t=18. From Fig.35 to Fig.40, the white circle means actual manipulator, the gray circle means imaginary manipulator 1 ($\tilde{\boldsymbol{q}}(t_1^*)$), the blue circle means imaginary manipulator 2 ($\tilde{\boldsymbol{q}}(t_2^*)$), the water color circle means imaginary manipulator 3 ($\tilde{\boldsymbol{q}}(t_3^*)$), and the green circle means total imaginary manipulator. In this simulation, we also set k_1=0.1, k_2=0.2, k_3=0.7. we think that imaginary manipulators and actual manipulator always keep a distance, and sometime, for example, t=12 or t=16, actual manipulator don't exist in colored circles, it means actual manipulator have lost high avoidance manipulability and safety.

Through Fig.41 to Fig.46, we also show AMSIP value distribution in case of predictive control from t=0 to t=18. We think the actual manipulator can always keep high avoidance manipulability in case of predictive control because the white circle (actual manipulator) is closer to colored area (high avoidance manipulability area). Indeed, predictive control has a possibility to be superior to multi-preview control.

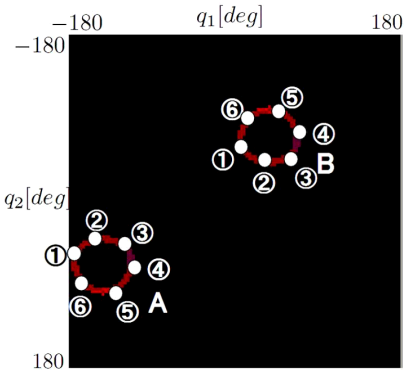

Fig. 17. AMSIP distribution

VII. CONCLUSION

In this paper, we explore the effectiveness of configuration prediction of redundant manipulator by using AMSIP value distribution. In the future, we need to show AMSIP value distribution in case of curve target trajectory to validate the effectiveness of predictive control. We will also consider more complex shape and curves of the workpieces for this numerical experiment. And a compensation method for the dynamical affections of the systems must be discussed.

REFERENCES

[1] Tongxiao Zhang, "Real-Time Configuration Control System for Redundant Manipulators and Analysis of Avoidance Space", A thesis for the degree of doctor of engineering, University of Fukui, pp.36-39, 2009.

[2] Yang Hou, Akira Yanou, Mamoru Minami, Yosuke Kobayashi, Satoshi Okazaki "Predictive Control of Redundant Manipulators based on Avoidance Manipulability", The 21th Intelligent System Symposium (FAN2011), 2011.

[3] Yang Hou, Akira Yanou, Mamoru Minami, Yosuke Kobayashi, Satoshi Okazaki "Analysis for Configuration Prediction of Redundant Manipulators based on Avoidance Manipulability", The 29th Annual Conference of the Robotics Society of Japan (RSJ2011), 2011.

[4] R. Findeisen and F. Allgower, An Introduction to Nonlinear Model Predictive Control, Proceeding of the Benelux Meeting on Systems and Control, pp.1-23, 2002.

[5] S. M. LaValle and J. J. Kuffner Jr., Randomized Kinodynamic Planning, International Journal of Robotics Research, Vol.20, No.5, pp.378-400, 2001.

[6] C. H. Kim, H. Tsujino and S. Sugano, Rapid Short-Time Path Planning for Phase Space, Journal of Robotics and Mechatronics, Vol.23, No.2, pp.271-280, 2011.

[7] Tongxiao Zhang, "Real-Time Configuration Control System for Redundant Manipulators and Analysis of Avoidance Space", A thesis for the degree of doctor of engineering, University of Fukui, pp.26-30, 2009.

[8] Hidekazu Suzuki, Mamoru Minami, "Visual Servoing to catch fish Using Global/local GA Search", IEEE/ASME Transactions on Mechatronics, Vol.10, Issue 3, 352-357, 2005.

[9] Hiroshi Tanaka, Mamoru Minami and Yasushi Mae, "Trajectory Tracking of Redundant Manipulators Based on Avoidance Manipulability Shape Index ", International Conference on Intelligent Robots and Systems, Edmonton, 2005, pp.1892-1897.

[10] Tsuneo Yoshikawa, "Foundations of Robot Control ", CORONA PUBLISHING CO., LTD.,1988.

[11] Homayoun Seraji, Bruce Bon "Real-Time Collsion Avoidance for Position-Controlled Manipulators", IEEE Transactions on Robotics and Automation, Vol.15, No.4, 1999, pp.670-677.

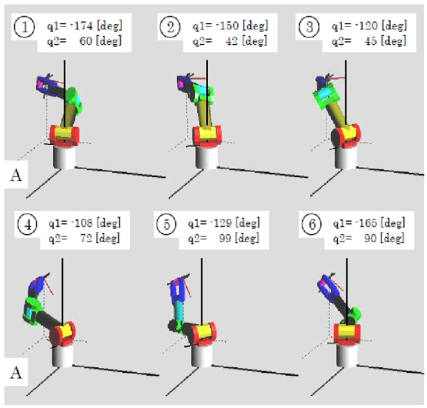

Fig. 18. Shape of Manipulator

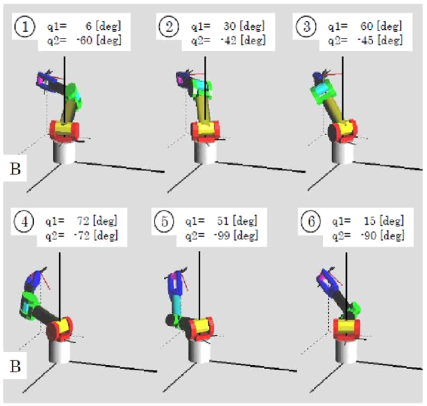

Fig. 19. Shape of Manipulator

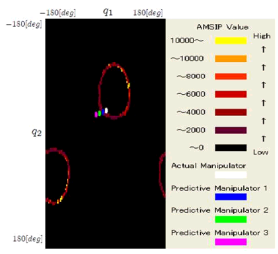

Fig. 20. AMSIP distribution of simulation

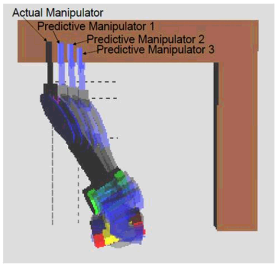

Fig. 21. Shape of manipulators of simulation

[12] Mamoru Minami, Yoshihiro Nomura, Toshiyuki Asakura "Avoidance Manipulability for Redundant Manipulators ", (in Japanese) Journal of the Robotics Society of Japan, Vol.17, No.6, 1999, pp.887-895.

[13] Bruno Siciliano and Jean-Jacques E. Slotine, "A General Framework for Managing Multiple Tasks in Highly Redundant Robotic Systems", *Fifth International Conference on Advanced Robotics*, Vol.2, 1991, pp.1211-1216.

[14] Mamoru Minami, Hidekasu Suzuki, Julien Agbanhan, "Fish Catching by Robot Using Gazing GA Visual Servoing", (in Japanese) Transactions of the Japan Society of Mechanical Engineers, Vol.68, No.668, 2002, pp.1198-1206.

[15] Keiji Ikeda, Hiroshi Tanaka, Tong-xiao Zhang, Mamoru Minami, Yasushi Mae "On-line Optimization of Avoidance Ability for Redundant Manipulator", International Conference on Intelligent Robots and Systems, Beijing, 2006, pp.592-597.

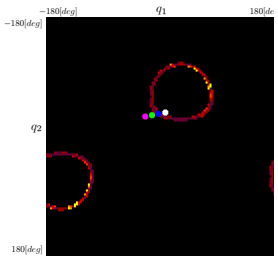

Fig. 22. AMSIP distribution when $t = 3[s]$

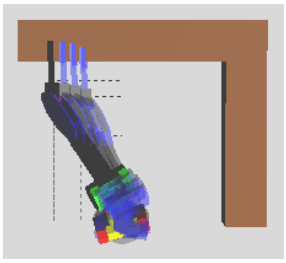

Fig. 23. Shape of manipulators when $t = 3[s]$

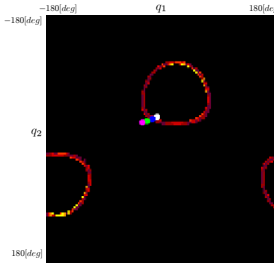

Fig. 24. AMSIP distribution when $t = 4.2[s]$

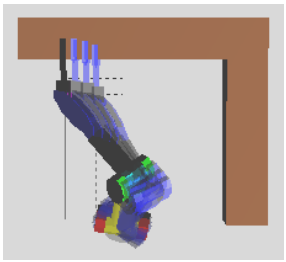

Fig. 25. Shape of manipulators when $t = 4.2[s]$

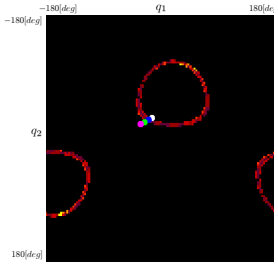

Fig. 26. AMSIP distribution when $t = 5.4[s]$

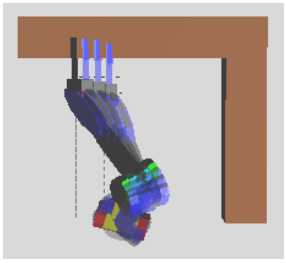

Fig. 27. Shape of manipulators when $t = 5.4[s]$

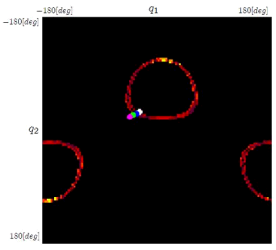

Fig. 28. AMSIP distribution when $t = 6.6[s]$

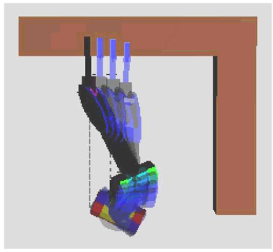

Fig. 29. Shape of manipulators when $t = 6.6[s]$

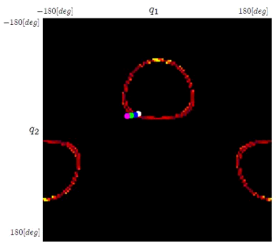

Fig. 30. AMSIP distribution when $t = 7.8[s]$

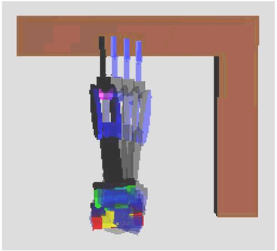

Fig. 31. Shape of manipulators when $t = 7.8[s]$

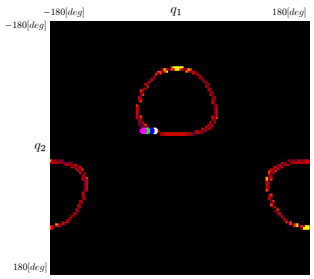

Fig. 32. AMSIP distribution when $t = 9[s]$

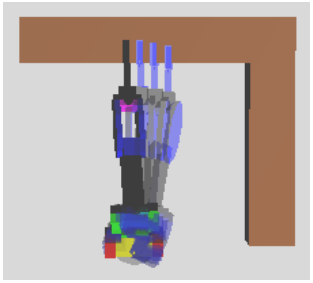

Fig. 33. Shape of manipulators when $t = 9[s]$

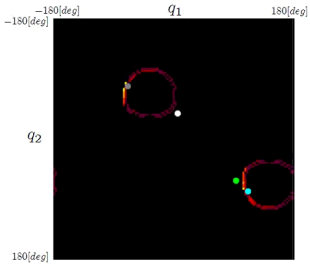

Fig. 39. AMSIP distribution when $t = 16[s]$

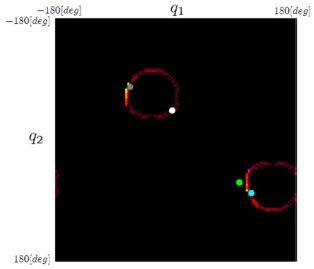

Fig. 40. AMSIP distribution when $t = 18[s]$

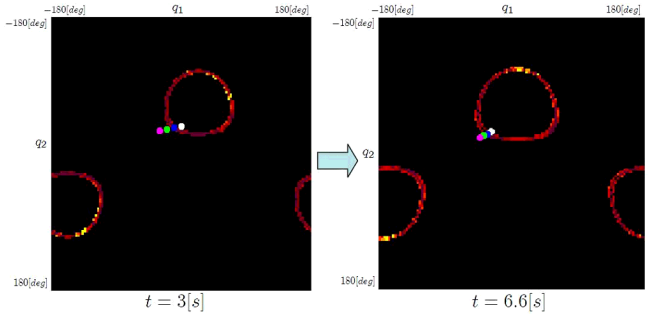

Fig. 34. Relation between prediction and actual situation of q_1 and q_2

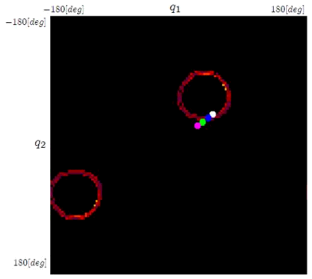

Fig. 41. AMSIP distribution when $t = 0[s]$

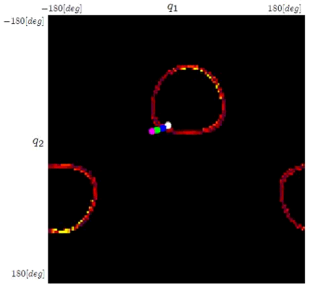

Fig. 42. AMSIP distribution when $t = 4[s]$

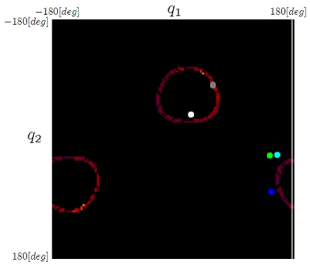

Fig. 35. AMSIP distribution when $t = 0[s]$

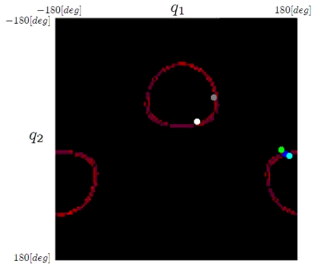

Fig. 36. AMSIP distribution when $t = 4[s]$

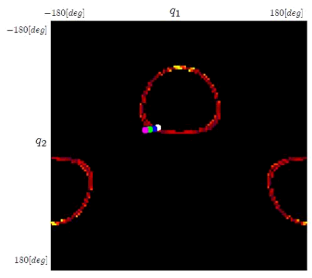

Fig. 43. AMSIP distribution when $t = 8[s]$

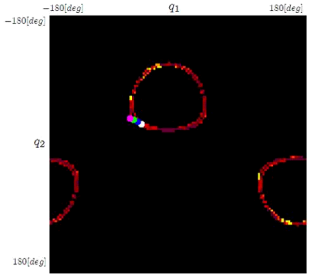

Fig. 44. AMSIP distribution when $t = 12[s]$

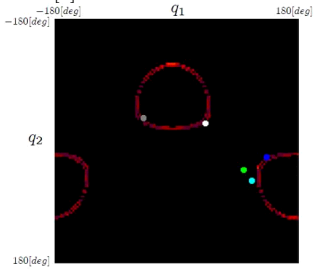

Fig. 37. AMSIP distribution when $t = 8[s]$

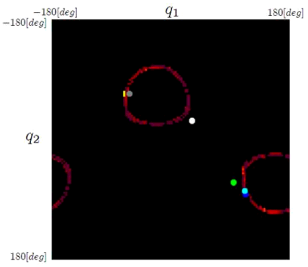

Fig. 38. AMSIP distribution when $t = 12[s]$

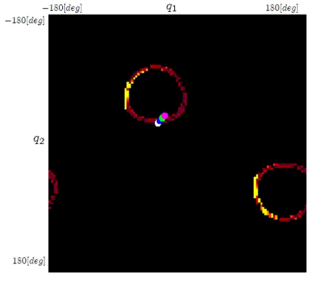

Fig. 45. AMSIP distribution when $t = 16[s]$

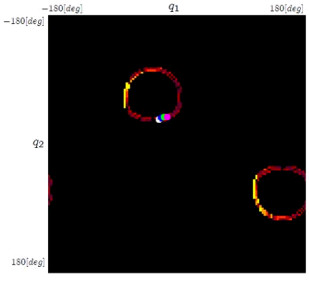

Fig. 46. AMSIP distribution when $t = 18[s]$